
SubIQ: Inverse Soft-Q Learning for Offline Imitation with Suboptimal Demonstrations

Huy Hoang^{1 2} Tien Mai^{1 2} Pradeep Varakantham^{1 2}

Abstract

We consider offline imitation learning (IL), which aims to mimic the expert’s behavior from its demonstration without further interaction with the environment. One of the main challenges in offline IL is dealing with the limited support of expert demonstrations that cover only a small fraction of the state-action spaces. In this work, we consider offline IL, where expert demonstrations are limited but complemented by a larger set of sub-optimal demonstrations of lower expertise levels. Most of the existing offline IL methods developed for this setting are based on behavior cloning or distribution matching, where the aim is to match the occupancy distribution of the imitation policy with that of the expert policy. Such an approach often suffers from over-fitting, as expert demonstrations are limited to accurately represent any occupancy distribution. On the other hand, since sub-optimal sets are much larger, there is a high chance that the imitation policy is trained towards sub-optimal policies. In this paper, to address these issues, we propose a new approach based on inverse soft-Q learning, where a *regularization* term is added to the training objective, with the aim of aligning the learned rewards with a pre-assigned reward function that allocates higher weights to state-action pairs from expert demonstrations, and lower weights to those from lower expertise levels. On standard benchmarks, our inverse soft-Q learning significantly outperforms other offline IL baselines by a large margin.

1. Introduction

Reinforcement learning (RL) has been raised as a strong framework for decision-making by its ability to learn by interacting with the environment. There are several appli-

cations in diverse domains: robotics (Kilinc & Montana, 2022; Hoang et al., 2023b), healthcare (Weng et al., 2017; Raghu et al., 2017), and structure generating (Dennis et al., 2020). However, to achieve high performance, original RL methods must balance the trade-off between exploration and exploitation. To handle this, several works utilize external support, such as expert demonstrations, to guide the learning scheme to achieve better performance, which is typically referred to as imitation learning (Ho & Ermon, 2016; Reddy et al., 2019; Garg et al., 2021; Hoang et al., 2023a).

Although having these assists, the number of interactions with the environment remains extremely large. Several works are trying to tackle the problem of offline schemes with a dataset of expert demonstrations (Wu et al., 2019a; Kumar et al., 2020; Zhang et al., 2021; Ajay et al., 2022). Starting with Behavioral Cloning (BC), it aims to maximize the likelihood of the expert’s decisions from the provided dataset. Although BC has a highly theoretical background that tends to converge towards expert behaviors, it often suffers from the distributional shift between the training dataset and the environment when there are insufficient demonstrations (Ross et al., 2011).

There are several works that aim to utilize non-expert demonstration datasets to reduce the reliance on a large number of expert demonstrations. This is a well-known approach in offline imitation learning, known as using supplementary data. However, it is obvious that directly applying BC to these larger supplementary datasets can lead to sub-optimal policies. Most prior work attempts to extract expert-like demonstrations from the supplementary dataset in order to expand the dataset available for Behavioral Cloning (Sasaki & Yamashina, 2020; Kim et al., 2021; 2022; Xu et al., 2022; Yu et al., 2023). However, these works assume expert demonstrations are present in the supplementary dataset and focus on identifying and utilizing those. The rest of the dataset is eliminated. On the other hand, we learn a Q function where the sub-optimal demonstrations also contribute to our understanding of the environment and ground truth reward function.

In this work, we aim to leverage ranked non-expert datasets to address the aforementioned issues and reduce the need for expert demonstrations. Our proposed approach is based

¹School of Computing and Information Systems ²Singapore Management University, Singapore. Correspondence to: Huy Hoang <mhhoang@smu.edu.sg>.

on inverse soft Q functions, incorporating a reward regularization term. This term is designed to align learning rewards with a predetermined reward function, assigning weights to state-action observations of varying expertise levels. It is worth noting that prior works (Brown et al., 2019; 2020; Chen et al., 2021) have also attempted to minimize the required demonstrations using ranked datasets by preference-based RL. However, their approaches are only applicable to online training.

Contributions: We make the following contributions:

- (i) We propose sub-IQ, a novel algorithm for *offline imitation learning with expert and non-expert demonstrations*.
- (ii) We provide key theoretical properties of the Sub-IQ objective function, which enable a scalable approach.
- (iii) To mitigate the *overestimation* issue, a common problem in offline Q learning, we develop a conservative version of Sub-IQ and demonstrate that the new objective is not only convex within the Q-space but also guarantees to return a Q function that lower-bounds its true value.
- (iv) We provide extensive experiments on two benchmark domains: *Mujoco* and *Panda-gym*, showing that our algorithms consistently outperform other existing algorithms.

1.1. Related Work

Imitation Learning. Imitation learning is recognized as a significant technique for learning from expert demonstrations. It begins with Behavioral Cloning (BC), which aims to maximize the likelihood of expert demonstrations. However, BC often underperforms in practice due to unforeseen scenarios (Ross et al., 2011). To overcome this limitation, Generative Adversarial Imitation Learning (GAIL) (Ho & Ermon, 2016) and Adversarial Inverse Reinforcement Learning (AIRL) (Fu et al., 2017) have been developed. These methods align the occupancy distributions of the policy and the expert within the Generative Adversarial Network (GAN) framework (Goodfellow et al., 2014). Alternatively, Soft Q Imitation Learning (SQIL) (Reddy et al., 2019) bypasses the complexities of adversarial training by assigning a reward of +1 to expert demonstrations and 0 to the others, subsequently learning a value function based on these rewards.

Offline Imitation Learning. While the aforementioned imitation learning algorithms show promise, they require interaction with the environment to obtain the policy distribution, which is often impractical. ValueDICE (Kostrikov et al., 2019) introduces a novel approach for off-policy training, suitable for offline training, using Stationary Distribution Corrections (Nachum et al., 2019a;b). However, ValueDICE necessitates adversarial training between the policy and the Q function, a challenge that O-NAIL (Arenz & Neumann, 2020) successfully addresses. Recently, algorithms like PWIL (Dadashi et al., 2021) and IQ-learn (Garg

et al., 2021) have utilized distribution distance, offering an alternative to adversarial training schemes. Since such approaches rely on occupancy distribution matching, a large expert dataset is often required to achieve the desired performance.

Learning from Imperfect Demonstration. Recent works have shown that utilizing imperfect demonstrations in online training schemes can provide additional information with several advantages. T-REX (Brown et al., 2019) and D-REX (Brown et al., 2020) have shown that understanding noise-ranked demonstrations as a reference-based approach can return a better policy without requiring expert demonstrations. Moreover, there are also several works (Wu et al., 2019b; Wang et al., 2021) that utilize the GAN framework (Goodfellow et al., 2014) for sub-optimal datasets and have achieved several successes.

Meanwhile, in the offline imitation learning context, from the sub-optimal demonstrations, TRAIL (Yang et al., 2021) use sup-optimal demonstrations to learn the environment’s dynamics using a feature encoder to map the high-dimensional state-action space into a lower dimension. This approach may face challenges in complex environments where predicting dynamics accurately is difficult. Other works assume that they can attract expert-like state-action pairs from the sub-optimal demonstration set and use them for BC with importance sampling (Sasaki & Yamashina, 2020; Xu et al., 2022; Yu et al., 2023; Kim et al., 2021; 2022). However, these studies must assume that expert state-actions are included in the sub-optimal set, which is not always the case. Additionally, expert-like state-actions may be misidentified, as reward information is not available. In contrast, our approach is more general, as *we do not assume that the sub-optimal set contains expert demonstrations*. We also allow for the inclusion of demonstrations of various qualities. Additionally, while prior works only recover expert policies, our approach enables the *recovery of both expert policies and rewards*, which facilitates applications in varied situations.

2. Background

Preliminaries. We consider a MDP define by the following tuple $\mathcal{M} = \langle S, A, r, P, \gamma, s_0 \rangle$, where S denotes the set of states, s_0 represents the initial state set, A is the set of actions, $r : S \times A \rightarrow \mathbb{R}$ defines the reward function for each state-action pair, and $P : S \times A \rightarrow S$ is the transition function, i.e., $P(s'|s, a)$ is the probability of reaching state $s' \in S$ when action $a \in A$ is made at state $s \in S$, and γ is a discount factor. In reinforcement learning (RL), the aim is to find a policy that maximizes the expected long-term

accumulated reward

$$\max_{\pi} \left\{ \mathbb{E}_{(s,a) \sim \rho_{\pi}} [r(s,a)] \right\}$$

where ρ_{π} is the occupancy measure of policy π , computed as. $\rho_{\pi}(s,a) = (1-\gamma)\pi(a|s) \sum_{t=1}^{\infty} \gamma^t P(s_t = s | \pi)$.

MaxEnt RL The MaxEnt RL framework aims to optimize a policy that maximizes an entropy regularized MDP

$$\max_{\pi} \mathbb{E}_{(s,a) \sim \rho_{\pi}} [r(s,a)] + H(\pi)$$

where $H(\pi)$ is an entropy regularizer, defined as a discounted causal entropy of the learning policy π , $H(\pi) = \mathbb{E}_{\rho_{\pi}} [-\log \pi(s,a)]$. The above MDP problem yields a unique solution π^* as $\pi^*(s,a) = \frac{e^{Q^*(s,a)}}{\sum_{a'} e^{Q^*(s,a')}}$, where the soft Q-function Q^* is a unique fixed point solution for the Bellman equations $\mathcal{B}_r[Q] = Q$, where

$$\begin{aligned} \mathcal{B}_r[Q](s,a) &= r(s,a) \\ &+ \gamma \mathbb{E}_{s' \sim P(s'|s,a)} \left[\log \left(\sum_{a'} e^{Q(s',a')} \right) \right] \end{aligned} \quad (1)$$

MaxEnt IRL In the context of IRL, the objective is to recover a reward function $r(s,a)$ from a set of expert demonstrations, \mathcal{D}^E . Let ρ^E be the occupancy measure of the expert policy. The MaxEnt IRL framework () proposes to recover the expert reward function by solving

$$\begin{aligned} \max_r \min_{\pi} \left\{ \mathbb{E}_{\rho^E} [r(s,a)] - (\mathbb{E}_{\rho_{\pi}} [r(s,a)] \right. \\ \left. - \mathbb{E}_{\rho_{\pi}} [\log \pi(s,a)]) \right\} \end{aligned} \quad (2)$$

Intuitively, we aim to find a reward function that achieves the highest difference between the expected value of the expert policy and the highest expected value among all other policies (computed through the min loop).

IQ-Learn Given a reward function r and a policy π , the soft Bellman equation is defined as

$$\mathcal{B}_r^{\pi}[Q](s,a) = r(s,a) + \gamma \mathbb{E}_{s'} [V^{\pi}(s')]$$

where $V^{\pi}(s) = \mathbb{E}_{a \sim \pi(a|s)} [Q(s,a) - \log \pi(a|s)]$. The Bellman equation $\mathcal{B}_r^{\pi}[Q] = Q$ is contractive and always yields a unique Q solution (Garg et al., 2021). In IQ-learn, they further define an inverse soft-Q Bellman operator

$$\mathcal{T}^{\pi}[Q] = Q(s,a) - \gamma \mathbb{E}_{s'} [V^{\pi}(s')]$$

where $V^{\pi}(s) = \mathbb{E}_{a \sim \pi(a|s)} [Q(s,a) - \log \pi(a|s)]$. (Garg et al., 2021) show that for any reward function $r(a,s)$, there is a unique Q^* function such that $\mathcal{B}_r^{\pi}[Q^*] = Q^*$, and for a Q^* function in the Q-space, there is a unique reward

function r such that $r = \mathcal{T}^{\pi}[Q^*]$. This result suggests that one can safely transform the objective function of the MaxEnt IRL from r -space to the Q-space as follows:

$$\begin{aligned} \max_Q \min_{\pi} \Phi(\pi, Q) &= \mathbb{E}_{\rho} [\mathcal{T}^{\pi}[Q](s,a)] \\ &- \mathbb{E}_{\rho_{\pi}} [\mathcal{T}^{\pi}[Q](s,a)] + \mathbb{E}_{\rho_{\pi}} [\log \pi(s,a)] \end{aligned} \quad (3)$$

which has several advantages; (Garg et al., 2021) show that $\Phi(\pi, Q)$ is convex in π and linear in Q , implying that (3) always yields a unique saddle point solution. In particular, (3) can be converted into a maximization over the Q-space, making the training problem no longer adversarial.

3. Inverse soft-Q Learning with Suboptimal Demonstrations

We now describe our inverse soft-Q learning approach where we have not just expert trajectories, but also multiple levels of sub-optimal trajectories. First, we formulate an *inverse soft-Q* objective function that enables matching the occupancy distribution of expert and sub-optimal demonstrations through inverting a soft-Q function. Second, to further enhance the learning and mitigate the effect of limited expert samples, we introduce a *regularization term* in the inverse soft-Q objective. This additional term is to align the learning rewards with a *pre-assigned* reward function that allocates higher values to state-action pairs from higher expertise levels. Third, we show that this new objective does not have the same advantageous properties as the one in IQ-Learn (Garg et al., 2021), and we provide a modification to the new objective, which is a lower bound and has all the important properties.

3.1. Formulation of Inverse Soft-Q Objective

We consider a setting where there are demonstrations classified into several sets of different expertise levels $\mathcal{D}^1, \mathcal{D}^2, \dots, \mathcal{D}^N$, where \mathcal{D}^1 consists of expert demonstrations and all the other sets contains sub-optimal ones. This setting is general and encompasses existing work in IL, which typically assumes that there are only two quality levels: expert and sub-optimal. Let $\mathcal{D} = \bigcup_{i \in [N]} \mathcal{D}^i$ be the union of all the demonstration sets and ρ^1, \dots, ρ^N be the occupancy measures of the respective expert policies. We then have an ordering of expected values across different levels of expert policies

$$\mathbb{E}_{\rho^1} [r^*(s,a)] > \mathbb{E}_{\rho^2} [r^*(s,a)] > \dots > \mathbb{E}_{\rho^N} [r^*(s,a)],$$

where $r^*(\cdot, \cdot)$ are the *ground-truth* rewards. Typically, we have the number of demonstrations in first level \mathcal{D}^1 is significantly lower than those from other expert levels, i.e.,

$$|\mathcal{D}^1| \ll |\mathcal{D}^i|, \text{ for } i = 2, \dots, N$$

The MaxEnt IRL objective from Equation 2 can be adapted to account for the multiple expert level setting as

$$\max_r \min_{\pi} \sum_{i \in [N]} w_i \mathbb{E}_{\rho^i} [r(s, a)] - \mathbb{E}_{\rho_{\pi}} [r(s, a)] + \mathbb{E}_{\rho_{\pi}} [\log \pi(s, a)] \quad (4)$$

where $w_i \geq 0$ is the weight associated with the expert level $i \in [N]$ and we have $w_1 > w_2 > \dots > w_N$ and $\sum_{i \in [N]} w_i = 1$. There are two key intuitions in the above optimization:

- (a) Expert level i accumulates higher expected values than expert levels greater than i ;
- (b) Difference in values accumulated by expert policies and the maximum of all other policies is maximized.

The optimization term can be rewritten as:

$$\mathbb{E}_{\rho^u} [r(s, a)] - \mathbb{E}_{\rho_{\pi}} [r(s, a)] - \mathbb{E}_{\rho_{\pi}} [\log \pi(s, a)],$$

where $\rho^u = \sum_{i \in [N]} w_i \rho^i$. Here we note that the expected reward $\sum_{i \in [N]} w_i \mathbb{E}_{\rho^i} [r(s, a)]$ is empirically approximated by samples from the demonstration sets $\mathcal{D}^1, \mathcal{D}^2, \dots, \mathcal{D}^N$, which may suffer from a low-sample size issue, as the number of samples in the best demonstration set \mathcal{D}^1 is *low*, so an empirical approximation of $\mathbb{E}_{\rho^1} [r(s, a)]$ using samples from \mathcal{D}^1 would be inaccurate. This is a foreseeable issue with any distributional matching approaches, especially when working with offline data without any online interactions. The primary challenge addressed in this section revolves around how to effectively utilize the optimal set of demonstrations \mathcal{D}^1 while mitigating the impact of low sample size.

3.2. Regularization with Reward Reference

To address the low-sample-size issue, we leverage the idea of the soft-Q Imitation Learning algorithm (Reddy et al., 2019). In this work, a reward reference of +1 is assigned to any state-action pair in the expert demonstrations, and the imitation is carried out by learning a policy that maximizes the expected accumulated pre-assigned rewards through soft-Q learning (so the learning policy will be trained towards replicating expert demonstrations). This approach would not suffer from a low-sample size issue and is more suitable to use with our inverse soft-Q approach, compared to other imitation learning algorithms that skip the reward inference step. To bring the idea into our context, we define a *reward reference* function $\bar{r}(s, a)$ such that $\bar{r}(s, a) > \bar{r}(s', a')$ for all (s, a) in \mathcal{D}^1 and $(s', a') \notin \mathcal{D}^1$, and $\bar{r}(s, a) > \bar{r}(s', a')$ for all (s, a) in \mathcal{D}^2 and $(s', a') \notin \mathcal{D}^2 \cup \mathcal{D}^1$, and so on. The aim here is to assign higher rewards to higher expert demonstrations, and zero rewards to those that do not belong to any demonstrations. Keeping this in mind, we incorporate a reward regularization term into the MaxEntIRL objective

in (4) as follows:

$$\max_r \min_{\pi} \left\{ K(r, \pi) \stackrel{def}{=} \underbrace{\sum_{i \in [N]} w_i \mathbb{E}_{\rho^i} [r(s, a)] - \mathbb{E}_{\rho_{\pi}} [r(s, a)]}_{\text{Occupancy matching}} + \underbrace{\mathbb{E}_{\rho_{\pi}} [\log \pi(s, a)]}_{\text{Entropy regularizer}} - \underbrace{\alpha \mathbb{E}_{\rho^u} [(r(s, a) - \bar{r}(s, a))^2]}_{\text{Reward regularizer}} \right\} \quad (5)$$

where $\alpha > 0$ is a weight parameter for the reward regularization term. With (5), the goal is to find a policy functions that match with the occupancy measure of the expert policies. Simultaneously, it ensures that the learning rewards are close to the pre-assigned rewards, aiming to guide the learning policy towards replicating expert demonstrations.

Even though (5) can be directly solved to recover rewards, prior research suggests that transforming (5) into the Q-space will enhance efficiency. We delve into this approach in the next section.

3.3. Tractable Lower-bound on Inverse Soft-Q

As discussed earlier, there is a one-to-one mapping between any reward function r and a function Q in the Q-space. Thus, the maximin problem in (5) can be equivalently transformed into the Q-space as:

$$\max_Q \min_{\pi} \left\{ \mathcal{H}(Q, \pi) \stackrel{def}{=} \sum_{i \in [N]} w_i \mathbb{E}_{\rho^i} [\mathcal{T}^{\pi}[Q](s, a)] - \mathbb{E}_{\rho_{\pi}} [\mathcal{T}^{\pi}[Q](s, a)] + \mathbb{E}_{\rho_{\pi}} [\log \pi(s, a)] - \alpha \mathbb{E}_{\rho^u} [(\mathcal{T}^{\pi}[Q](s, a) - \bar{r}(s, a))^2] \right\} \quad (6)$$

where $r(s, a)$ is replaced by $\mathcal{T}^{\pi}[Q](s, a)$ and

$$\mathcal{T}^{\pi}[Q](s, a) = Q(s, a) - \gamma \mathbb{E}_{s'} [V^{\pi}(s')]$$

$$V^{\pi}(s) = \mathbb{E}_{a \sim \pi(a|s)} [Q(s, a) - \log \pi(a|s)]$$

In the context of single-expert-level, (Garg et al., 2021) demonstrated that the objective function in the Q-space is concave in Q and convex in π , implying that the maximin problem always has a unique saddle point solution. Moreover, the inner minimization problem over π will yield a unique closed-form solution, enabling the transformation of the maximin problem into a non-adversarial concave problem within the Q-space. This makes the inverse soft-Q problem advantageous to handle. However, in our context, *these results do not hold*. Let us first state the following proposition, which asserts that $\mathcal{H}(Q, \pi)$ is not necessarily concave in π .

Proposition 3.1. $\mathcal{H}(Q, \pi)$ is concave in Q but is not convex in π .

In general, we can see that the first and second term of (7) are convex in Q , but the reward regularizer term, which can be written as $\alpha \mathbb{E}_{\rho^u} \left[Q(s, a) - \bar{r}(s, a) - \mathbb{E}_{s' \sim P(\cdot|s,a)} \mathbb{E}_{a' \sim \pi(\cdot|s')} (Q(s', a') - \log \pi(s', a'))^2 \right]$, is not concave (or concave) in π (details are shown in the Appendix). The property indicated in Proposition 3.1 implies that the maximin problem within the Q -space $\max_Q \min_{\pi} J(Q, \pi)$ may not have a unique saddle point solution and would be more challenging to solve, compared to the original inverse IQ-learn problem. Additionally, to circumvent non-adversarial training, (Garg et al., 2021) demonstrated that the inner minimization problem in π always has a closed-form solution such that $\pi^Q = \operatorname{argmax}_{\pi} V^{\pi}(s)$ for all $s \in S$. This result is essential to convert the minimax problem into a concave maximization problem in Q . Unfortunately, this result does not hold with the new objective function in (7), as shown below:

Proposition 3.2. $\mathcal{H}(Q, \pi)$ may not necessarily be minimized at π^* such that $\pi^* = \operatorname{argmax}_{\pi} V^{\pi}(s)$, for all $s \in S$.

To overcome the above challenges, our approach involves constructing a more tractable objective function that lower-boundedly approximates the objective of (7). To this end, let us first define $\Gamma(Q) = \min_{\pi} \mathcal{H}(Q, \pi)$. We then look at the regularization term, which causes all the aforementioned challenges, and write:

$$\begin{aligned} (\mathcal{T}^{\pi}[Q](s, a) - \bar{r}(s, a))^2 &= (Q(s, a) - \bar{r}(s, a) - \mathbb{E}_{s'}[V^{\pi}(s')])^2 \\ &= (Q(s, a) - \bar{r}(s, a))^2 + (\mathbb{E}_{s'}[V^{\pi}(s')])^2 + \\ &\quad 2(\bar{r}(s, a) - Q(s, a))\mathbb{E}_{s'}[V^{\pi}(s')] \end{aligned}$$

We then take out the negative part of $(\bar{r}(s, a) - Q(s, a))$ using ReLU, and consider a slightly new objective function as follows:

$$\begin{aligned} \hat{\mathcal{H}}(Q, \pi) &\stackrel{def}{=} \sum_{i \in [N]} w_i \mathbb{E}_{\rho^i} [\mathcal{T}^{\pi}[Q](s, a)] \\ &\quad - (\mathbb{E}_{\rho_{\pi}} [\mathcal{T}^{\pi}[Q](s, a)] - \mathbb{E}_{\rho_{\pi}} [\log \pi(s, a)]) \\ &\quad - \alpha \mathbb{E}_{\rho^u} \left[(Q(s, a) - \bar{r}(s, a))^2 + (\mathbb{E}_{s'} V^{\pi}(s'))^2 \right. \\ &\quad \left. + 2\operatorname{ReLU}(\bar{r}(s, a) - Q(s, a))\mathbb{E}_{s'} V^{\pi}(s') \right] \end{aligned} \quad (7)$$

Let $\hat{\Gamma}(Q) = \min_{\pi} \hat{\mathcal{H}}(Q, \pi)$. The following proposition indicates that $\hat{\Gamma}(Q)$ always lower-bounds $\Gamma(Q)$.

Proposition 3.3. For any $Q \geq 0$, we have $\hat{\Gamma}(Q) \leq \Gamma(Q)$ and $\max_Q \hat{\Gamma}(Q) \leq \max_Q \Gamma(Q)$. Moreover, $\Gamma(Q) = \hat{\Gamma}(Q)$ if $Q(s, a) \leq \bar{r}(s, a)$ for all (s, a) .

We note that assuming $Q \geq 0$ is not restrictive, as if the expert's rewards $r^*(s, a)$ are non-negative (typically the case), then the soft-Q function should also be non-negative. This is due to the fact that $Q(s, a) = \mathbb{E}[\sum_{s_t, a_t} \gamma^t (r(s, a) - \log \pi(s, a)) | (s_0, a_0) = (s, a)] \geq 0$. As $\hat{\Gamma}(Q)$ provides

a lower-bound approximation of $\Gamma(Q)$, maximizing $\hat{\Gamma}(Q)$ over the Q -space would drive $\Gamma(Q)$ towards its maximum value. It is important to note that, given that the inner problem involves minimization, obtaining an upper-bound approximation function is easier. However, since the outer problem is a maximization one, an upper bound would not be helpful in guiding the resulting solution towards optimal ones.

The following theorem indicates that, in fact, the approximation $\hat{\Gamma}(Q)$ is more tractable to use.

Theorem 3.4. For any $Q \geq 0$, the following results hold

- (i) The inner minimization problem $\min_{\pi} \hat{\mathcal{H}}(Q, \pi)$ has a unique optimal solution π^Q such that $\pi^Q = \operatorname{argmin}_{\pi} V^{\pi}(s)$ for all $s \in S$ and $\pi^Q(a|s) = \frac{\exp(Q(s, a))}{\sum_a \exp(Q(s, a))}$.
- (ii) $\max_{\pi} V^{\pi}(s) = \log(\sum_a \exp(Q(s, a))) \stackrel{def}{=} V^Q(s)$.
- (iii) $\hat{\Gamma}(Q)$ is concave for $Q \geq 0$

The above theorem tells us that new objective $\hat{\Gamma}(Q)$ has a closed form where $V^{\pi}(s)$ are replaced by $V^Q(s)$. Moreover $\hat{\Gamma}(Q)$ is concave for all $Q \geq 0$. The concavity is particularly advantageous, as it guarantees that the optimization objective is well-behaved and has a unique solution Q^* such that (Q^*, π^{Q^*}) form a unique saddle point of $\max_Q \min_{\pi} \hat{\mathcal{H}}(Q, \pi)$.

4. Practical Algorithm – SubIQ

The term $\mathbb{E}_{\rho_{\pi}} [\mathcal{T}^{\pi}[Q](s, a)] - \mathbb{E}_{\rho_{\pi}} [\log \pi(s, a)]$ can be written as (Garg et al., 2021):

$$\begin{aligned} \mathbb{E}_{\rho_{\pi}} [\mathcal{T}^{\pi}[Q](s, a)] - \mathbb{E}_{\rho_{\pi}} [\log \pi(s, a)] &= (1 - \gamma) \mathbb{E}_{s_0} [V^{\pi}(s_0)] \\ &= \mathbb{E}_{\rho^*} [V^{\pi}(s) - \gamma \mathbb{E}_{s'} V^{\pi}(s')] \end{aligned}$$

for any valid occupancy measure ρ^* . So, for any policy occupancy measure, we can write this term through the union of expert policies ρ^u as

$$\begin{aligned} \mathbb{E}_{\rho_{\pi}} [\mathcal{T}^{\pi}[Q](s, a)] - \mathbb{E}_{\rho_{\pi}} [\log \pi(s, a)] &= \\ &= \sum_{i \in [N]} w_i \mathbb{E}_{\rho^i} [V^{\pi}(s) - \gamma \mathbb{E}_{s'} V^{\pi}(s')] \end{aligned} \quad (8)$$

As a result, by replacing $V^{\pi}(s)$ with $V^Q(s)$, we can write $\hat{\Gamma}(Q)$ in a compact form as

$$\begin{aligned} \hat{\Gamma}(Q) &= \sum_{i \in [N]} w_i \mathbb{E}_{\rho^i} [Q(s, a) - \gamma \mathbb{E}_{s'} V^Q(s')] \\ &\quad - \sum_{i \in [N]} \mathbb{E}_{\rho^i} [V^Q(s) - \gamma \mathbb{E}_{s'} V^Q(s')] \\ &\quad - \alpha \sum_{i \in [N]} w_i \mathbb{E}_{\rho^i} [\Delta_{\bar{r}}^Q(s, a)] \end{aligned} \quad (9)$$

where $\Delta_{\bar{r}}^Q(s, a) = (Q(s, a) - \bar{r}(s, a))^2 + (\mathbb{E}_{s'} V^Q(s'))^2 + 2\text{ReLU}(\bar{r}(s, a) - Q(s, a))\mathbb{E}_{s'} V^Q(s)$.

Empirical expectation estimates. In an empirical offline implementation, to maximize $\hat{\mathcal{H}}(Q)$, samples (s, a, s') from demonstrations can be used to approximate the expectations over ρ^i : $\sum_{(s,a,s') \in \mathcal{D}^i} [Q(s, a) - \gamma V^Q(s')]$, $\sum_{(s,a,s') \in \mathcal{D}^i} [V^Q(s) - \gamma V^Q(s')]$, and $\sum_{(s,a) \in \mathcal{D}^i} [\Delta_{\bar{r}}^Q(s, a)]$. We note that in continuous-action controls, the computation of $V^Q(s)$ involves a sum over infinitely many actions, which is impractical. In this case, we can update both Q and π in a soft actor-critic (SAC) manner. That is, for each π , we update Q towards $\max_Q \{\hat{\mathcal{H}}(Q, \pi)\}$ and for each Q , we update π to bring it towards π^Q by solving $\max_{\pi} \{V^{\pi}(s)\}$, for all s . As shown above, $\hat{\mathcal{H}}(Q, \pi)$ is concave in Q and $V^{\pi}(s)$ is convex in π , so we can expect this SAC will exhibit good behavior and stability.

Estimating the Reward Reference. The reward reference function $\bar{r}(s, a)$ is a critical component of our learning algorithm. In the following, we outline our approach to automatically infer such a reward function from demonstrations of different expertise levels. The general idea is to learn a function that assigns higher values to higher expert-level demonstrations. To achieve this, let us define $R(\tau) = \sum_{(s,a) \in \tau} \bar{r}(s, a)$ (i.e., accumulated reward of trajectory τ). For two trajectories τ_i, τ_j , let $\tau_i \prec \tau_j$ denote that τ_i is lower in quality compared to τ_j (i.e., τ_i belongs to demonstrations from lower-expert policies, compared to τ_j). We model the probability $P(\tau_i \prec \tau_j)$ by a softmax-normalized (or binary logit) distribution, which gives:

$$P(\tau_i \prec \tau_j) = \frac{\exp(R(\tau_j))}{\exp(R(\tau_i)) + \exp(R(\tau_j))}$$

Intuitively, increasing $R(\tau_i)$ will lower $P(\tau_i \prec \tau_j)$ and $P(\tau_i \prec \tau_j) < 0.5$ if $R(\tau_i) < R(\tau_j)$. Having this, we use the following loss function:

$$\min_{\bar{r}} \left\{ \mathcal{L}(\bar{r}) = \sum_{i \in [N]} \sum_{(s,a),(s',a') \in \mathcal{D}^i} (\bar{r}(s, a) - \bar{r}(s', a'))^2 - \sum_{\substack{h,k \in [N], h < k \\ \tau_i \in \mathcal{D}^h, \tau_j \in \mathcal{D}^k}} \ln P(\tau_i \prec \tau_j) + \phi(\bar{r}) \right\} \quad (10)$$

Here, the first term of $\mathcal{L}(\bar{r})$ serves to guarantee that the reward reference values for (s, a) pairs within the same demonstration group are similar, and the second term aims to increase the likelihood that the accumulated rewards of trajectories adhere to the expert-level order, and the last term is a convex regularizer. Importantly, it can be shown below that $\mathcal{L}(\bar{r})$ is convex in \bar{r} , making the learning well-behaved.

Proposition 4.1. $\mathcal{L}(\bar{r})$ is strictly convex in \bar{r} .

In practice, one can model $\bar{r}(s, a)$ by a neural network of parameters θ and optimize $\mathcal{L}(\theta)$ over θ -space.

Conservative soft-Q learning Over-estimation is a common issue in offline Q-learning due to out-of-distribution actions and function approximation errors (Fujimoto et al., 2018). We also observe this in our IL context. To overcome this issue and enhance stability, we leverage the approach in (Kumar et al., 2020) to enhance our inverse soft-Q learning. The aim is to learn a *conservative* soft-Q function that lower-bounds its true value. We formulate the *conservative inverse soft-Q* objective as:

$$\max_Q \left\{ \hat{\mathcal{H}}^C(Q, \pi) = -\beta \sum_{\substack{s \sim \mathcal{D} \\ a \sim \mu(a|s)}} [Q(s, a)] + \hat{\mathcal{H}}(Q, \pi) \right\} \quad (11)$$

where $\mu(a|s)$ is a particular state-action distribution. We note that in (11), the *conservative* term is added to the objective function, while in the conservative Q-learning algorithm (Kumar et al., 2020), this term is added to the Bellman error objective of each Q-function update. This difference makes the theory developed in (Kumar et al., 2020) not applicable. In Proposition 4.2 below, we show that solving $\max_Q \hat{\mathcal{H}}^C(Q)$ will always yield a Q-function that is a lower bound to the Q function obtained by solving $\max_Q \hat{\mathcal{H}}(Q, \pi)$.

Proposition 4.2. Let $\hat{Q} = \text{argmax}_Q \hat{\mathcal{H}}(Q, \pi)$ and $\hat{Q}^C = \text{argmax}_Q \hat{\mathcal{H}}^C(Q, \pi)$, we have

$$\sum_{\substack{s \sim \mathcal{D} \\ a \sim \mu(a|s)}} \hat{Q}^C(s, a) \leq \sum_{\substack{s \sim \mathcal{D} \\ a \sim \mu(a|s)}} \hat{Q}(s, a)$$

We can adjust the scale parameter β to regulate the conservativeness of the objective. Intuitively, if we optimize Q over a lower-bounded Q-space, increasing the scale parameter β will force each $Q(s, a)$ towards its lower bound. Consequently, when β is sufficiently large, \hat{Q}^C will point-wise lower-bound \hat{Q} , i.e., $\hat{Q}^C(s, a) \leq \hat{Q}(s, a)$ for all (s, a) .

5. Experiments

5.1. Experiment Setup

Baselines. We compare our sub-IQ with state-of-the-art algorithms in offline IL with sub-optimal demonstrations: TRAIL (Yang et al., 2021), DemoDICE (Kim et al., 2021), and DWBC (Xu et al., 2022). Moreover, we also compare with other IL baselines: BC with only sub-optimal datasets (BC-O), BC with only expert data (BC-E), BC with all datasets (BC-both), and BC with fixed weight for

Table 1: Comparison results for *Mujoco* and *Panda-gym* tasks. Values falling within the range of the best score $\pm 2\%$ are emphasized in **bold**.

	Cheetah	Ant	Walker	Hopper	Humanoid	Reach	Push	PnP	Slide
BC-E	-3.2±0.9	6.4±19.1	0.3±0.4	8.3±4.1	1.3±0.2	13.9±5.9	8.2±3.8	3.7±2.7	0.0±0.0
BC-O	14.2±2.9	35.2±20.1	66.1±10.8	16.7±4.0	10.6±6.3	16.2±5.5	8.8±4.5	3.9±2.7	0.1±0.3
BC-both	13.2±3.6	47.0±5.9	63.9±7.3	22.6±12.8	9.0±3.5	16.3±5.0	9.0±4.3	4.4±3.0	0.1±0.4
W-BC	12.9±2.8	47.3±6.4	58.6±9.1	20.9±6.6	19.6±19.0	15.7±5.1	8.8±4.3	3.7±2.8	0.0±0.0
TRAIL	-4.1±0.3	-4.7±1.9	0.2±0.3	1.1±0.5	2.6±0.6	18.3±5.1	11.7±4.0	7.8±3.7	1.7±1.8
IQ	-3.4±0.6	-3.4±1.3	0.1±0.7	0.3±0.2	2.4±0.6	97.7±2.4	26.3±10.9	18.1±12.5	0.1±0.4
SQIL	-5.0±0.7	-33.8±7.4	0.2±0.2	0.2±0.0	0.9±0.1	22.1±15.1	9.6±3.3	3.2±2.9	0.1±0.3
DemoDICE	0.4±2.0	31.7±8.9	7.2±3.1	18.7±7.5	2.6±0.8	14.0±5.3	8.1±3.7	4.3±2.4	0.1±0.5
DWBC	-0.2±2.5	10.4±5.0	25.1±16.3	66.0±20.9	3.7±0.3	93.4±4.3	36.9±7.4	25.0±6.3	11.6±4.4
SQRF (ours)	46.8±14.0	78.8±6.2	90.2±6.8	59.9±21.5	5.7±1.1	99.2±0.8	72.7±5.2	66.5±7.6	36.6±7.0
A-IQ (ours)	7.8±2.7	76.6±5.2	71.3±24.6	25.2±18.5	4.7±1.1	99.0±1.1	76.8±4.4	68.9±6.3	39.1±6.2
Sub-IQ (ours)	68.1±3.0	77.5±4.9	93.8±3.1	65.2±29.2	68.1±10.9	99.8±0.9	70.0±6.8	70.8±6.7	42.8±6.6

Algorithm 1 SubIQ: Inverse soft-Q Learning with Sub-optimal Demonstrations

Require: $(\mathcal{D}^1, \mathcal{D}^2, \dots, \mathcal{D}^N), (w_1, w_2, \dots, w_N), \bar{r}_\eta, Q_\psi, \pi_\theta, \phi$
estimate reward reference function
for iteration $i \dots N_e$ **do**
 $d \leftarrow (d^1, d^1, \dots, d^N) \sim (\mathcal{D}^1, \mathcal{D}^2, \dots, \mathcal{D}^N)$
from dataset d , calculate $\mathcal{L}(\bar{r}_\eta)$ by (10)
 $\eta \leftarrow \eta - \nabla_\eta \mathcal{L}(\bar{r}_\eta)$
end for
train Sub-IQ
for iteration $i \dots N$ **do**
 $d \leftarrow (d^1, d^1, \dots, d^N) \sim (\mathcal{D}^1, \mathcal{D}^2, \dots, \mathcal{D}^N)$
Update Q function
from dataset d , calculate $\hat{\mathcal{H}}^C(Q_\psi, \pi_\theta)$ by (11)
 $\psi \leftarrow \psi + \nabla_\psi \hat{\mathcal{H}}^C(Q_\psi, \pi_\theta)$
Update policy for actor-critic
 $\theta \leftarrow \theta + \nabla [\mathbb{E}_{a \sim \pi_\theta(a|s)} [Q_\psi(s, a) - \ln(\pi_\theta(a|s))]]$
end for

each dataset (W-BC), SQIL (Reddy et al., 2019), and IQ-learn (Garg et al., 2021) with only expert data¹. In particular, since TRAIL, DemoDICE, and DWBC were designed to work with only two datasets (one expert and one supplementary), we combine all the sub-optimal datasets into one single supplementary dataset. Meanwhile, BC-E, BC-O, and BC-both combine all available data into a large dataset for learning, while W-BC optimizes $\sum_i \mathbb{E}_{s, a \sim \mathcal{D}^i} w_i \ln(\pi(a|s))$. We also provide comparison results with two variants of our sub-IQ: (i) A-IQ (adaptive IQ-learn), derived by retaining the first and second terms of our primary objective (7), and (ii) SQRF (soft-Q learning with reward reference), obtained by retaining only the last term of (7). The aim is to assess

¹The performances of SQIL and IQlearn with both expert and sub-optimal data are much worse

how the *distribution matching* and *reward regularization* terms help each other to achieve better performance in our sub-IQ. Here we note that the conservative Q-learning term is employed in both sub-IQ and the two variants to enhance stability. Without this term, these algorithms exhibit much worse performance and are highly unstable.

Environments and Data Generation : We test on five Mujoco tasks (Todorov et al., 2012) and four arm manipulation tasks from Panda-gym (Gallouédec et al., 2021). The maximum number of (s, a) per trajectory is 1000 for the Mujoco and is 50 for Panda-gym tasks (descriptions in Appendix B.1). In our main experiments reported below, we test with three expertise levels (i.e., one expert and two sup-optimal datasets). Experiments with more and less expertise levels will be provided in the Appendix. The sub-optimal demonstrations have been generated by randomly adding noise to expert actions and interacting with the environments. More details of these generated datasets can be found in the Appendix B.3.

Metric: The return has been normalized by the formula $\text{score} = \frac{\text{return} - \text{R.return}}{\text{E.return} - \text{R.return}} \times 100$ where R.return is the mean return of random policy and E.return is the mean return of the expert policy. The scores are calculated by taking the last ten evaluation scores of each seed, with at least five seeds per report.

Comparison settings. In the following, we will conduct experiments to evaluate the following aspects: (i) performance comparison between our algorithms and other imitation learning baselines mentioned earlier, (ii) the influence of augmenting expert data, and (iii) the impact of sub-optimal demonstrations. Additional experiments can be found in the Appendix.

5.2. Main Comparison Results

Table 1 shows comparison results for our methods and 9 different baselines across five *Mujoco* tasks and four *Panda-gym* tasks. From lowest to highest expertise levels, we randomly sample (25k-10k-1k) trajectories for *Mujoco* tasks and (10k-5k-100) transitions for *Panda-gym* tasks for every seed (details of these three-level dataset are provided in Appendix B.3). In general, Sub-IQ performs the best on 8 out of the 9 tasks, and is competitive for the other task. Surprisingly, SQRF’s performance is quite comparable compared to Sub-IQ for several tasks. However, it faces difficulties in *Humanoid* tasks where its performance is remarkably low. None of the BC variants do well, except for the Walker (easiest *Mujoco* task). Furthermore, TRAIL’s performance is poor, indicating that it struggles to learn accurate dynamics using sub-optimal data. In addition, SQIL and IQ-learn also struggle with limited expert data. Moreover, our SQRF is better than SQIL, highlighting the benefits of learning with reward references instead of simply assigning +1 to every expert transition.

5.3. Augmented Expert Demonstrations

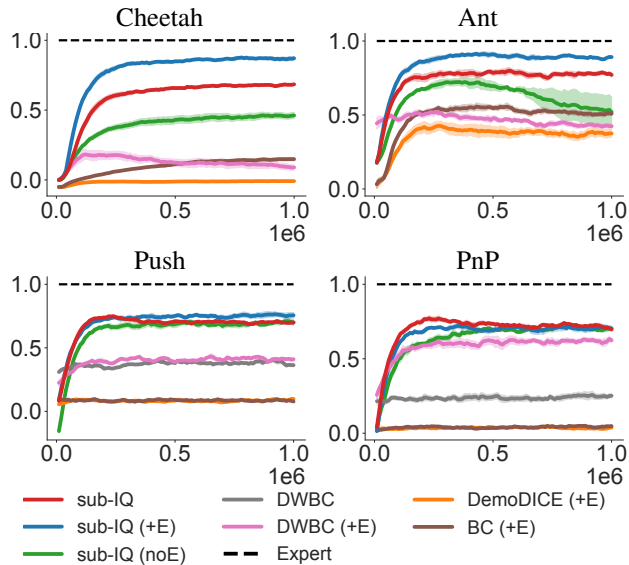


Figure 1: Comparison results with additional expert demonstrations; (+E) signifies that the expert dataset is increased from 1k to 5k for *Mujoco* and from 100 to 500 for *Panda-gym*, while (noE) indicates no expert data.

We aim to assess the performance of sub-IQ with augmented expert data. To this end, we use two *Mujoco* and two *Panda-gym* tasks, keeping the same sup-optimal data and add more expert demonstrations to the training sets. The comparison results are reported in Figure 1. For the *Mujoco* tasks, which are more difficult, adding more expert trajectories significantly enhances the performance of all the algorithms. How-

ever, for the two *Panda-gym* tasks, the influence of adding more expert data appears to be less significant in Push and completely absent in PnP. This would be because expert trajectories in these tasks are typically short, consisting of only 2-7 transitions. Hence, a larger quantity of additional expert data may be required to enhance performance.

5.4. Impact of Sup-optimal Demonstrations

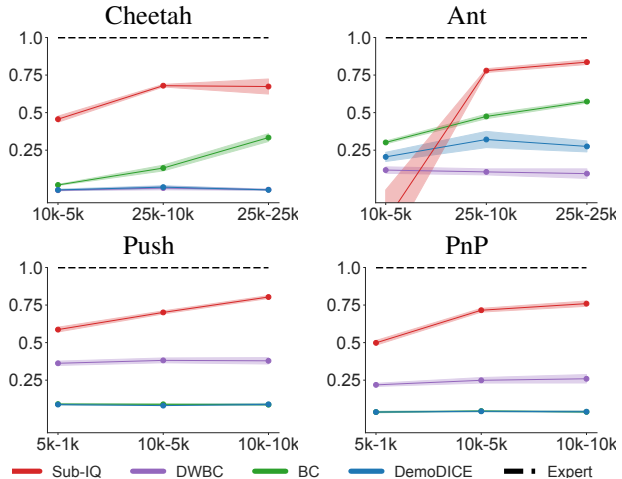


Figure 2: Performance comparisons with varied sub-optimal data sizes. The x -axis shows the size of Level 2 and 3 sup-optimal datasets, and y -axis shows the scores.

We present numerical results to assess the impact of sub-optimal data on the performance of our sub-IQ and other baselines. To this end, we keep the same expert dataset and adjust the non-expert data used in Table 1. The performance is reported in Fig.2. It is evident that reducing the amount of data in sub-optimal datasets can result in a significant degradation in the performance of our Sub-IQ and the other baselines. Conversely, adding more sub-optimal data can enhance overall stability and lead to improved performance. More detailed results can be found in Appendix B.4.

6. Conclusion

In this paper, we have developed sub-IQ, a novel non-adversarial inverse soft-Q learning algorithm for offline imitation learning from expert and sub-optimal demonstrations. We have demonstrated that our algorithm possesses several favorable properties, contributing to its well-behaved, stable, and scalable nature. Additionally, we have devised a preference-based loss function to automate the estimation of reward reference values. We have provided extensive experiments based on several benchmark tasks, demonstrating the ability of our *sub-IQ* algorithm to leverage both expert and non-expert data to achieve superior performance compared to state-of-the-art algorithms.

7. Broader Impacts

This paper investigates offline imitation learning with supplementary data, and our algorithms are tested on simulated tasks. Although this paper does not have immediate, direct social impacts, the potential practical applications of our research could lead to positive societal changes. By extending the applicability of imitation learning algorithms, our work may support the development of more efficient solutions in areas like robotics, autonomous vehicles, education, and healthcare. However, it is important to acknowledge that the misuse of such technology could result in negative consequences, such as manipulating information to influence people’s behavior or privacy. Hence, it is imperative to remain vigilant in ensuring that imitation learning techniques are utilized in a responsible and ethical manner.

References

- Ajay, A., Du, Y., Gupta, A., Tenenbaum, J. B., Jaakkola, T. S., and Agrawal, P. Is conditional generative modeling all you need for decision making? In *The Eleventh International Conference on Learning Representations*, 2022.
- Arenz, O. and Neumann, G. Non-adversarial imitation learning and its connections to adversarial methods. *arXiv preprint arXiv:2008.03525*, 2020.
- Boyd, S. P. and Vandenberghe, L. *Convex optimization*. Cambridge university press, 2004.
- Brown, D., Goo, W., Nagarajan, P., and Niekum, S. Extrapolating beyond suboptimal demonstrations via inverse reinforcement learning from observations. In *International conference on machine learning*, pp. 783–792. PMLR, 2019.
- Brown, D. S., Goo, W., and Niekum, S. Better-than-demonstrator imitation learning via automatically-ranked demonstrations. In *Conference on robot learning*, pp. 330–359. PMLR, 2020.
- Chen, L., Paleja, R., and Gombolay, M. Learning from sub-optimal demonstration via self-supervised reward regression. In *Conference on robot learning*, pp. 1262–1277. PMLR, 2021.
- Dadashi, R., Hussenot, L., Geist, M., and Pietquin, O. Primal wasserstein imitation learning. In *ICLR*, 2021.
- Dennis, M., Jaques, N., Vinitzky, E., Bayen, A., Russell, S., Critch, A., and Levine, S. Emergent complexity and zero-shot transfer via unsupervised environment design. *Advances in neural information processing systems*, 33: 13049–13061, 2020.
- Fu, J., Luo, K., and Levine, S. Learning robust rewards with adversarial inverse reinforcement learning. *arXiv preprint arXiv:1710.11248*, 2017.
- Fujimoto, S., Hoof, H., and Meger, D. Addressing function approximation error in actor-critic methods. In *International conference on machine learning*, pp. 1587–1596. PMLR, 2018.
- Gallouédec, Q., Cazin, N., Dellandréa, E., and Chen, L. panda-gym: Open-source goal-conditioned environments for robotic learning. *arXiv preprint arXiv:2106.13687*, 2021.
- Garg, D., Chakraborty, S., Cundy, C., Song, J., and Ermon, S. Iq-learn: Inverse soft-q learning for imitation. *Advances in Neural Information Processing Systems*, 34: 4028–4039, 2021.
- Goodfellow, I., Pouget-Abadie, J., Mirza, M., Xu, B., Warde-Farley, D., Ozair, S., Courville, A., and Bengio, Y. Generative adversarial nets. *Advances in neural information processing systems*, 27, 2014.
- Ho, J. and Ermon, S. Generative adversarial imitation learning. *Advances in neural information processing systems*, 29, 2016.
- Hoang, H., Mai, T., and Varakantham, P. Imitate the good and avoid the bad: An incremental approach to safe reinforcement learning. *arXiv preprint arXiv:2312.10385*, 2023a.
- Hoang, M.-H., Dinh, L., and Nguyen, H. Learning from pixels with expert observations. *arXiv preprint arXiv:2306.13872*, 2023b.
- Kilinc, O. and Montana, G. Reinforcement learning for robotic manipulation using simulated locomotion demonstrations. *Machine Learning*, pp. 1–22, 2022.
- Kim, G.-H., Seo, S., Lee, J., Jeon, W., Hwang, H., Yang, H., and Kim, K.-E. Demodice: Offline imitation learning with supplementary imperfect demonstrations. In *International Conference on Learning Representations*, 2021.
- Kim, G.-H., Lee, J., Jang, Y., Yang, H., and Kim, K.-E. Lobsdice: Offline learning from observation via stationary distribution correction estimation. *Advances in Neural Information Processing Systems*, 35:8252–8264, 2022.
- Kostrikov, I., Nachum, O., and Tompson, J. Imitation learning via off-policy distribution matching. In *International Conference on Learning Representations*, 2019.
- Kumar, A., Zhou, A., Tucker, G., and Levine, S. Conservative q-learning for offline reinforcement learning.

- Advances in Neural Information Processing Systems*, 33: 1179–1191, 2020.
- Nachum, O., Chow, Y., Dai, B., and Li, L. Dualdice: Behavior-agnostic estimation of discounted stationary distribution corrections. *Advances in neural information processing systems*, 32, 2019a.
- Nachum, O., Dai, B., Kostrikov, I., Chow, Y., Li, L., and Schuurmans, D. Algaedice: Policy gradient from arbitrary experience. *arXiv preprint arXiv:1912.02074*, 2019b.
- Raghu, A., Komorowski, M., Ahmed, I., Celi, L., Szolovits, P., and Ghassemi, M. Deep reinforcement learning for sepsis treatment. *arXiv preprint arXiv:1711.09602*, 2017.
- Reddy, S., Dragan, A. D., and Levine, S. Sqil: Imitation learning via reinforcement learning with sparse rewards. *arXiv preprint arXiv:1905.11108*, 2019.
- Ross, S., Gordon, G., and Bagnell, D. A reduction of imitation learning and structured prediction to no-regret online learning. In *Proceedings of the fourteenth international conference on artificial intelligence and statistics*, pp. 627–635. JMLR Workshop and Conference Proceedings, 2011.
- Sasaki, F. and Yamashina, R. Behavioral cloning from noisy demonstrations. In *International Conference on Learning Representations*, 2020.
- Todorov, E., Erez, T., and Tassa, Y. Mujoco: A physics engine for model-based control. In *2012 IEEE/RSJ international conference on intelligent robots and systems*, pp. 5026–5033. IEEE, 2012.
- Wang, Y., Xu, C., Du, B., and Lee, H. Learning to weight imperfect demonstrations. In *International Conference on Machine Learning*, pp. 10961–10970. PMLR, 2021.
- Weng, W.-H., Gao, M., He, Z., Yan, S., and Szolovits, P. Representation and reinforcement learning for personalized glycemic control in septic patients. *arXiv preprint arXiv:1712.00654*, 2017.
- Wu, Y., Tucker, G., and Nachum, O. Behavior regularized offline reinforcement learning. *ArXiv*, abs/1911.11361, 2019a. URL <https://api.semanticscholar.org/CorpusID:208291277>.
- Wu, Y.-H., Charoenphakdee, N., Bao, H., Tangkaratt, V., and Sugiyama, M. Imitation learning from imperfect demonstration. In *International Conference on Machine Learning*, pp. 6818–6827. PMLR, 2019b.
- Xu, H., Zhan, X., Yin, H., and Qin, H. Discriminator-weighted offline imitation learning from suboptimal demonstrations. In *Proceedings of the 39th International Conference on Machine Learning*, pp. 24725–24742, 2022.
- Yang, M., Levine, S., and Nachum, O. Trail: Near-optimal imitation learning with suboptimal data. In *International Conference on Learning Representations*, 2021.
- Yu, L., Yu, T., Song, J., Neiswanger, W., and Ermon, S. Offline imitation learning with suboptimal demonstrations via relaxed distribution matching. In *Proceedings of the AAAI conference on artificial intelligence*, volume 37, pp. 11016–11024, 2023.
- Zhang, C., Kuppannagari, S. R., and Prasanna, V. K. Brac+: Improved behavior regularized actor critic for offline reinforcement learning. *ArXiv*, abs/2110.00894, 2021. URL <https://api.semanticscholar.org/CorpusID:238259485>.

A. Missing Proofs

Proposition 3.1 $J(Q, \pi)$ is concave in Q but is not convex in π .

Proof. We recall that

$$J(Q, \pi) = \sum_{i \in [N]} w_i \mathbb{E}_{\rho^i} [\mathcal{T}^\pi[Q](s, a)] - \mathbb{E}_{\rho^\pi} [\mathcal{T}^\pi[Q](s, a)] - \mathbb{E}_{\rho^\pi} [\log \pi(s, a)] - \alpha \mathbb{E}_{\rho^\pi} [(\mathcal{T}^\pi[Q](s, a) - \bar{r}(s, a))^2] \quad (12)$$

where $\mathcal{T}^\pi[Q](s, a) = Q(s, a) - \gamma \mathbb{E}_{s' \sim P(s'|s, a)} [V^\pi(s')]$ and $V^\pi(s) = \mathbb{E}_{a \sim \pi(a|s)} [Q(s, a) - \log \pi(a|s)]$. We see that $\mathcal{T}^\pi[Q](s, a)$ is linear in Q for any (s, a) . Thus, the first and second terms of $J(Q, \pi)$ in (12) are linear in Q . The last term of (12) involves a sum of squares of linear functions of Q , which are convex. So, $J(Q, \pi)$ is concave in Q .

To see that $J(Q, \pi)$ is generally not convex in π , we will consider a quadratic component of the reward regularization term $(\mathcal{T}^\pi[Q](s, a) - \bar{r}(s, a))^2$ and show that there is an instance of Q and \bar{r} values that makes this term convex. We first write:

$$\begin{aligned} \mathcal{T}^\pi[Q](s, a) - \bar{r}(s, a) &= Q(s, a) - \gamma \sum_{s'} P(s'|s, a) V^\pi(s') - \bar{r}(s, a) \\ &= Q(s, a) - \gamma \sum_{s'} P(s'|s, a) \sum_{a''} \pi(a''|s') (Q(s', a'') - \log \pi(a''|s')) - \bar{r}(s, a) \end{aligned}$$

For simplification, let us choose $Q(s', a'') = 0$ for all s' such that $P(s'|s, a) > 0$. This allows us to simplify $\mathcal{T}^\pi[Q](s, a) - \bar{r}(s, a)$ as

$$\mathcal{T}^\pi[Q](s, a) - \bar{r}(s, a) = \gamma \sum_{s'} P(s'|s, a) \sum_{a''} \pi(a''|s') \log \pi(a''|s') + Q(s, a) - \bar{r}(s, a)$$

We further see that, for any $s \in S$, $\sum_{a \in A} \pi(a|s) \log \pi(a|s)$ achieves its minimum value at $\pi(a|s) = 1/|A|$ for all $a \in |A|$, and $\sum_{a \in A} \pi(a|s) \log \pi(a|s) \geq \log 1/|A|$ for any policy π . As a result we have:

$$\gamma \sum_{s'} P(s'|s, a) \sum_{a''} \pi(a''|s') \log \pi(a''|s') \geq \gamma \log \frac{1}{|A|}$$

So if we select $Q(s, a)$ such that $Q(s, a) - \bar{r}(s, a) - \gamma \log |A| \geq 0$, then $\mathcal{T}^\pi[Q](s, a) - \bar{r}(s, a) \geq 0$ for any π . Now we consider the quadratic function $\Gamma(\pi) = (\lambda(\pi))^2$ where $\lambda(\pi) = \mathcal{T}^\pi[Q](s, a) - \bar{r}(s, a)$. Since each term $\pi(a'') \log \pi(a''|s')$ is convex in π , $\lambda(\pi)$ is convex in π . To show $\Gamma(\pi)$ is convex in π , we will show that for any two policies π_1, π_2 and $\alpha \in [0, 1]$, $\Gamma(\alpha\pi_1 + (1 - \alpha)\pi_2) \leq \alpha\Gamma(\pi_1) + (1 - \alpha)\Gamma(\pi_2)$. To this end, we write

$$\begin{aligned} \alpha\Gamma(\pi_1) + (1 - \alpha)\Gamma(\pi_2) &\stackrel{(a)}{\geq} (\alpha\lambda(\pi_1) + (1 - \alpha)\lambda(\pi_2))^2 \\ &\stackrel{(b)}{\geq} (\lambda(\alpha\pi_1 + (1 - \alpha)\pi_2))^2 \\ &= \Gamma(\alpha\pi_1 + (1 - \alpha)\pi_2) \end{aligned}$$

where (a) is because the function $h(t) = t^2$ is convex in t , and (b) is because

- (i) $\alpha\lambda(\pi_1) + (1 - \alpha)\lambda(\pi_2) \geq \lambda(\alpha\pi_1 + (1 - \alpha)\pi_2)$ (as $\lambda(\pi)$ is convex in π)
- (ii) $\alpha\lambda(\pi_1) + (1 - \alpha)\lambda(\pi_2)$ and $\lambda(\alpha\pi_1 + (1 - \alpha)\pi_2)$ are both non-negative, and function $h(t) = t^2$ is increasing for all $t \geq 0$.

So, we see that with the Q values chosen above, function $(\mathcal{T}^\pi[Q](s, a) - \bar{r}(s, a))^2$ is convex and $-\alpha(\mathcal{T}^\pi[Q](s, a) - \bar{r}(s, a))^2$ is concave. So, intuitively, when α is sufficiently large, $J(Q, \pi)$ would be almost concave (so not convex), which is the desired result. \square

Proposition 3.2 $J(Q, \pi)$ may not necessarily be minimized at π_Q such that $\pi_Q = \operatorname{argmax}_\pi V^\pi(s)$, for all $s \in S$.

Proof. We first write $J(Q, \pi)$ as

$$\begin{aligned} J(Q, \pi) &= \sum_{i \in [N]} w_i \mathbb{E}_{\rho^i} [\mathcal{T}^\pi [Q](s, a)] - \mathbb{E}_{\rho_\pi} [\mathcal{T}^\pi [Q](s, a)] - \mathbb{E}_{\rho_\pi} [\log \pi(s, a)] \\ &\quad - \alpha \mathbb{E}_{\rho^u} [(\mathcal{T}^\pi [Q](s, a) - \bar{r}(s, a))^2] \\ &= \sum_{i \in [N]} w_i \mathbb{E}_{\rho^i} [Q(s, a) - \gamma \mathbb{E}_{s'} V^\pi(s')] - (1 - \gamma) \mathbb{E}_{s_0} V^\pi(s_0) \\ &\quad - \alpha \mathbb{E}_{\rho^u} [(Q(s, a) - \bar{r}(s, a) - \gamma \mathbb{E}_{s'} V^\pi(s'))^2] \end{aligned} \quad (13)$$

We then see that the terms $\mathbb{E}_{\rho^i} [Q(s, a) - \gamma \mathbb{E}_{s'} V^\pi(s')]$ and $-\gamma \mathbb{E}_{s_0} V^\pi(s_0)$ are minimized (over π) when $V^\pi(s)$, for all s , are maximized. We will prove that it would not be the case for the last term. Let us choose Q and \bar{r} such that $Q(s, a) - \bar{r}(s, a) > \gamma \mathbb{E}_{s'} V^{\pi_Q}(s')$. We see that for any policy $\pi \neq \pi_Q$, we have

$$\begin{aligned} Q(s, a) - \bar{r}(s, a) &> \gamma \mathbb{E}_{s'} V^{\pi_Q}(s') \geq \mathbb{E}_{s'} V^\pi(s') \\ \text{Thus, } Q(s, a) - \bar{r}(s, a) - V^\pi(s') &\geq Q(s, a) - \bar{r}(s, a) - V^{\pi_Q}(s') > 0 \end{aligned}$$

which implies that

$$-\alpha \mathbb{E}_{\rho^u} [(Q(s, a) - \bar{r}(s, a) - \gamma \mathbb{E}_{s'} V^{\pi_Q}(s'))^2] \leq -\alpha \mathbb{E}_{\rho^u} [(Q(s, a) - \bar{r}(s, a) - \gamma \mathbb{E}_{s'} V^\pi(s'))^2]$$

So the last term of (13) would not be minimized at $\pi = \pi_Q$. In fact, in the above scenario, this last term will be maximized at $\pi = \pi_Q$. As a result, there is always α sufficiently large such that the last term significantly dominates the other terms and $J(Q, \pi)$ is not minimized at $\pi = \pi_Q$. \square

Proposition 3.3 For any $Q \geq 0$, we have $\hat{\Gamma}(Q) \leq \Gamma(Q)$ and $\max_{Q \geq 0} \hat{\Gamma}(Q) \leq \max_{Q \geq 0} \Gamma(Q)$. Mover, $\Gamma(Q) = \hat{\Gamma}(Q)$ if $Q(s, a) \leq \bar{r}(s, a)$ for all s, a .

Proof. We first write $\hat{\mathcal{H}}(Q, \pi)$ as

$$\begin{aligned} \hat{\mathcal{H}}(Q, \pi) &= \sum_{i \in [N]} w_i \mathbb{E}_{\rho^i} [\mathcal{T}^\pi [Q](s, a)] - \mathbb{E}_{\rho_\pi} [\mathcal{T}^\pi [Q](s, a)] - \mathbb{E}_{\rho_\pi} [\log \pi(s, a)] \\ &\quad - \alpha \mathbb{E}_{\rho^u} \left[(Q(s, a) - \bar{r}(s, a))^2 + (\mathbb{E}_{s'} V^\pi(s'))^2 + 2\operatorname{ReLU}(\bar{r}(s, a) - Q(s, a)) \mathbb{E}_{s'} V^\pi(s) \right] \end{aligned} \quad (14)$$

Since $Q \geq 0$, $V^\pi(s) = \mathbb{E}_{a \sim \pi(\cdot|s)} [Q(s, a) - \log \pi(a|s)] \geq 0$. Thus $2\operatorname{ReLU}(\bar{r}(s, a) - Q(s, a)) \mathbb{E}_{s'} V^\pi(s) \geq 2(\bar{r}(s, a) - Q(s, a)) \mathbb{E}_{s'} V^\pi(s)$. As a result, the last term of $\hat{\mathcal{H}}(Q, \pi)$ is bounded as

$$\begin{aligned} &-\alpha \mathbb{E}_{\rho^u} \left[(Q(s, a) - \bar{r}(s, a))^2 + (\mathbb{E}_{s'} V^\pi(s'))^2 + 2\operatorname{ReLU}(\bar{r}(s, a) - Q(s, a)) \mathbb{E}_{s'} V^\pi(s) \right] \\ &\leq -\alpha \mathbb{E}_{\rho^u} \left[(Q(s, a) - \bar{r}(s, a))^2 + (\mathbb{E}_{s'} V^\pi(s'))^2 - 2(Q(s, a) - \bar{r}(s, a)) \mathbb{E}_{s'} V^\pi(s) \right] \\ &= -\alpha \mathbb{E}_{\rho^u} [(\mathcal{T}^\pi [Q](s, a) - \bar{r}(s, a))^2] \end{aligned}$$

It then follows that $\hat{\mathcal{H}}(Q, \pi) \leq J(Q, \pi)$. Thus, $\min_\pi \hat{\mathcal{H}}(Q, \pi) \leq \min_\pi J(Q, \pi)$ or $\hat{\Gamma}(Q) \leq \Gamma(Q)$. Mover, we see that if $\bar{r}(s, a) \geq Q(s, a)$ for all (s, a) , then $2\operatorname{ReLU}(\bar{r}(s, a) - Q(s, a)) \mathbb{E}_{s'} V^\pi(s) = 2(\bar{r}(s, a) - Q(s, a)) \mathbb{E}_{s'} V^\pi(s)$, implying that $\hat{\mathcal{H}}(Q, \pi) = J(Q, \pi)$ and $\hat{\Gamma}(Q) = \Gamma(Q)$. This completes the proof. \square

Theorem 3.4 For any $Q \geq 0$, the following results hold

(i) The inner minimization problem $\min_{\pi} \widehat{\mathcal{H}}(Q, \pi)$ has a unique optimal solution π^* such that $\pi^Q = \operatorname{argmin}_{\pi} V^{\pi}(s)$ for all $s \in S$ and

$$\pi^Q(a|s) = \frac{\exp(Q(s, a))}{\sum_a \exp(Q(s, a))}.$$

(ii) $\max_{\pi} V^{\pi}(s) = \log(\sum_a \exp(Q(s, a))) \stackrel{\text{def}}{=} V^Q(s)$.

(iii) $\widehat{\Gamma}(Q)$ is concave for $Q \geq 0$

Proof. We first rewrite the formulation of $\widehat{\mathcal{H}}(Q, \pi)$ as

$$\begin{aligned} \widehat{\mathcal{H}}(Q, \pi) &= \sum_{i \in [N]} w_i \mathbb{E}_{\rho^i} [Q(s, a) - \gamma \mathbb{E}_{s'} V^{\pi}(s')] - (1 - \gamma) \mathbb{E}_{s_0} V^{\pi}(s_0) \\ &\quad - \alpha \mathbb{E}_{\rho^u} \left[(Q(s, a) - \bar{r}(s, a))^2 + (\mathbb{E}_{s'} V^{\pi}(s'))^2 + 2 \operatorname{ReLU}(\bar{r}(s, a) - Q(s, a)) \mathbb{E}_{s'} V^{\pi}(s) \right] \end{aligned}$$

We then see that the first and second term of $\widehat{\mathcal{H}}(Q, \pi)$ are minimized when $V^{\pi}(s)$ are minimized, i.e., at $\pi = \pi_Q$. For the last term, since $V^{\pi}(s) \geq 0$ (because $Q \geq 0$), $-(\mathbb{E}_{s'} V^{\pi}(s'))^2$ and $-2 \operatorname{ReLU}(\bar{r}(s, a) - Q(s, a)) \mathbb{E}_{s'} V^{\pi}(s)$ are also minimized at $\pi = \pi_Q$. So, $\widehat{\mathcal{H}}(Q, \pi)$ is minimized at $\pi = \pi_Q$ as desired.

(ii) is already proved in (Garg et al., 2021).

For (iii), we rewrite $\widehat{\mathcal{H}}(Q, \pi)$ as

$$\begin{aligned} \widehat{\mathcal{H}}(Q, \pi) &= \sum_{i \in [N]} w_i \mathbb{E}_{\rho^i} [\mathcal{T}^{\pi}[Q](s, a)] - (1 - \gamma) \mathbb{E}_{s_0, a \sim \pi(a|s_0)} [Q(s_0, a) - \log \pi(a|s_0)] \\ &\quad - \alpha \mathbb{E}_{\rho^u} \left[(\bar{r}(s, a) - Q(s, a) + \mathbb{E}_{s'} V^{\pi}(s))^2 \right] + \alpha \mathbb{E}_{\rho^u} \left[(\min\{0, \bar{r}(s, a) - Q(s, a)\}) \right] \\ &= \sum_{i \in [N]} w_i \mathbb{E}_{\rho^i} [\mathcal{T}^{\pi}[Q](s, a)] - (1 - \gamma) \mathbb{E}_{s_0, a \sim \pi(a|s_0)} [Q(s_0, a) - \log \pi(a|s_0)] \\ &\quad - \alpha \mathbb{E}_{\rho^u} \left[(\bar{r}(s, a) - Q(s, a) + \mathbb{E}_{s'} V^{\pi}(s))^2 \right] + \alpha \mathbb{E}_{\rho^u} \left[(\min\{0, \bar{r}(s, a) - Q(s, a)\}) \right] \end{aligned} \quad (15)$$

Then, the first and second terms of (15) is linear in Q . The fourth term is concave. For third term, let $\Phi(Q) = |\bar{r}(s, a) - Q(s, a)| + \mathbb{E}_{s'} V^{\pi}(s)$. We see that $\Phi(Q) \geq 0$ for any $Q \geq 0$ and $\Phi(Q)$ is convex in Q (because $V^{\pi}(s)$ is linear in Q). It then follows that, for any $\eta \in [0, 1]$ and $Q_1, Q_2 \geq 0$, we have

$$\begin{aligned} \eta(\Phi(Q))^2 + (1 - \eta)(\Phi(Q))^2 &\stackrel{(a)}{\geq} (\eta\Phi(Q) + (1 - \eta)\Phi(Q))^2 \\ &\stackrel{(b)}{\geq} (\Phi(\eta Q_1 + (1 - \eta)Q_2))^2 \end{aligned} \quad (16)$$

where (a) is due to the fact function $h(t) = t^2$ is convex, and (b) is because $h(t) = t^2$ is non-decreasing for all $t \geq 0$, and $\Phi(Q)$ is convex and always takes non-negative values. The last inequality in(16) implies that $(\Phi(Q))^2$ is convex in Q . So the last term of (15) is concave in Q . Putting all together we conclude that $\widehat{\mathcal{H}}(Q, \pi)$ is concave in Q as desired. \square

Proposition 4.1 $\mathcal{L}(\bar{r})$ is strictly convex in \bar{r} .

Proof. We first write $\mathcal{L}(\bar{r})$ as

$$\mathcal{L}(\bar{r}) = \sum_{i \in [N]} \sum_{(s,a),(s',a') \in \mathcal{D}^i} (\bar{r}(s,a) - \bar{r}(s',a'))^2 - \sum_{\substack{h,k \in [N], h < k \\ \tau_i \in \mathcal{D}^h, \tau_j \in \mathcal{D}^k}} \ln \frac{\exp(R(\tau_j))}{\exp(R(\tau_j)) + \exp(R(\tau_i))} + \phi(\bar{r}) \quad (17)$$

$$= \sum_{i \in [N]} \sum_{(s,a),(s',a') \in \mathcal{D}^i} (\bar{r}(s,a) - \bar{r}(s',a'))^2 - \sum_{\substack{h,k \in [N], h < k \\ \tau_i \in \mathcal{D}^h, \tau_j \in \mathcal{D}^k}} \left(R(\tau_j) - \ln(\exp(R(\tau_j)) + \exp(R(\tau_i))) + \phi(\bar{r}) \right) \quad (18)$$

We then see that the first term is a sum of squares of linear functions of \bar{r} , thus is strictly convex. Moreover, since $R(\tau_i)$ is linear in \bar{r} for any τ_i , the term $\ln(\exp(R(\tau_i)) + \exp(R(\tau_j)))$ has a log-sum-exp form. So this term is convex as well (Boyd & Vandenberghe, 2004). Putting all together we see that $\mathcal{L}(\bar{r})$ is strictly convex in \bar{r} as desired. \square

Proposition 4.2 Let $\hat{Q} = \operatorname{argmax}_Q \hat{\mathcal{H}}(Q, \pi)$ and $\hat{Q}^C = \operatorname{argmax}_Q \hat{\mathcal{H}}^C(Q, \pi)$, we have

$$\sum_{\substack{s \sim \mathcal{D} \\ a \sim \mu(a|s)}} \hat{Q}^C(s, a) \leq \sum_{\substack{s \sim \mathcal{D} \\ a \sim \mu(a|s)}} \hat{Q}(s, a)$$

Proof. We write

$$\hat{\mathcal{H}}^C(\hat{Q}^C, \pi) = -\beta \sum_{\substack{s \sim \mathcal{D} \\ a \sim \mu(a|s)}} \hat{Q}^C(s, a) + \hat{\mathcal{H}}(\hat{Q}^C, \pi) \quad (19)$$

$$\stackrel{(a)}{\geq} -\beta \sum_{\substack{s \sim \mathcal{D} \\ a \sim \mu(a|s)}} \hat{Q}(s, a) + \hat{\mathcal{H}}(\hat{Q}, \pi)$$

$$\stackrel{(b)}{\geq} -\beta \sum_{\substack{s \sim \mathcal{D} \\ a \sim \mu(a|s)}} \hat{Q}(s, a) + \hat{\mathcal{H}}(\hat{Q}^C, \pi) \quad (20)$$

where (a) is because $\hat{Q}^C = \operatorname{argmax}_Q \hat{\mathcal{H}}^C(Q, \pi)$ and (b) is because $\hat{\mathcal{H}}(\hat{Q}, \pi) \geq \hat{\mathcal{H}}(\hat{Q}^C, \pi)$. Combine (19) and (20) we get

$$\beta \sum_{\substack{s \sim \mathcal{D} \\ a \sim \mu(a|s)}} \hat{Q}^C(s, a) \leq \beta \sum_{\substack{s \sim \mathcal{D} \\ a \sim \mu(a|s)}} \hat{Q}(s, a)$$

as desired. \square

B. Experimental Details

B.1. Environment

B.1.1. MUJOCO

MuJoCo gym environments (Todorov et al., 2012) like HalfCheetah, Ant, Walker2d, Hopper, and Humanoid are integral to the field of reinforcement learning (RL), particularly in the domain of continuous control and robotics:

- **HalfCheetah**: This environment simulates a two-dimensional cheetah-like robot. The objective is to make the cheetah run as fast as possible, which involves learning complex, coordinated movements across its body.
- **Ant**: This environment features a four-legged robot resembling an ant. The challenge is to control the robot to move effectively, balancing stability and speed.
- **Walker2d**: This environment simulates a two-dimensional bipedal robot. The goal is to make the robot walk forward as fast as possible without falling over.

- **Hopper:** The Hopper environment involves a single-legged robot. The primary challenge is to balance and hop forward continuously, which requires maintaining stability while in motion.
- **Humanoid:** The Humanoid environment is among the most complex, featuring a bipedal robot with a human-like structure. The task involves mastering various movements, from walking to more complex maneuvers, while maintaining balance.

An expert is trying to maximize the reward function by moving with a trajectory length limit of 1000. All five environments are shown in Figure 3.

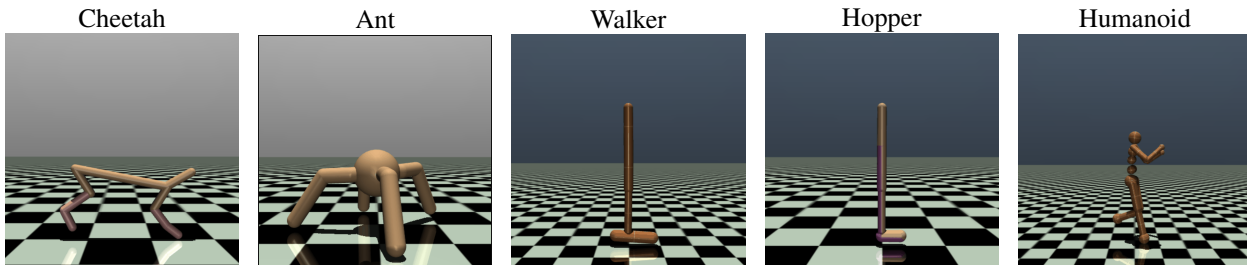


Figure 3: Five different Mujoco environments.

B.1.2. PANDA-GYM

The *Panda-gym* environments (Gallouédec et al., 2021), designed for the Franka Emika Panda robot in reinforcement learning, include *PandaReach*, *PandaPush*, *PandaPickandPlace*, and *PandaSlide*. Here’s a short description of each:

- **PandaReach:** The task is to move the robot’s gripper to a randomly generated target position within a specific volume. It focuses on precise control of the gripper’s movement.
- **PandaPush:** In this environment, a cube placed on a table must be pushed to a target position. The gripper remains closed, emphasizing the robot’s ability to manipulate objects through pushing actions.
- **PandaPickandPlace:** This more complex task involves picking up a cube and placing it at a target position above the table. It requires coordinated control of the robot’s gripper for both lifting and accurate placement.
- **PandaSlide:** Here, the robot must slide a flat object (like a hockey puck) to a target position on a table. The gripper is fixed in a closed position, and the task demands imparting the right amount of force to slide the object to the target.

In these environments, the reward function is -1 for every time step it has not finished the task. Moreover, the maximum horizon is extremely short, with a maximum of 50, while an expert can complete the task after several steps. All four different environments are shown in Figure 4.

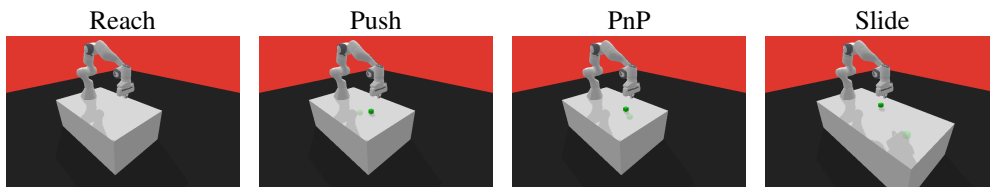


Figure 4: Five different Panda-gym environments.

B.2. Algorithm Overview

The Figure 5 provide the overview of our algorithm.

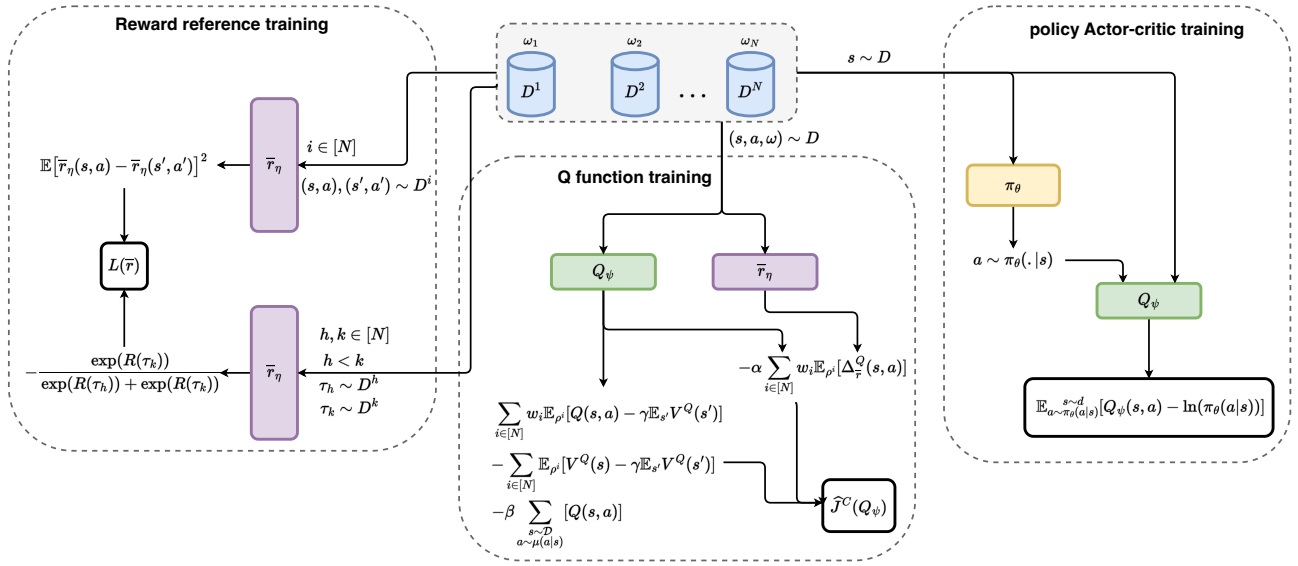


Figure 5: Overview of Sub-IQ.

B.3. Qualities of the Generated Expert and Non-Expert Datasets

We create sub-optimal datasets by adding noise to actions of the expert policy and let them interact with the environments to collect the sub-optimal trajectories. Each task has its own difficulty and sensitivity to the noise of the actions. The averaged returns of the generated datasets are reported in Figure 6.

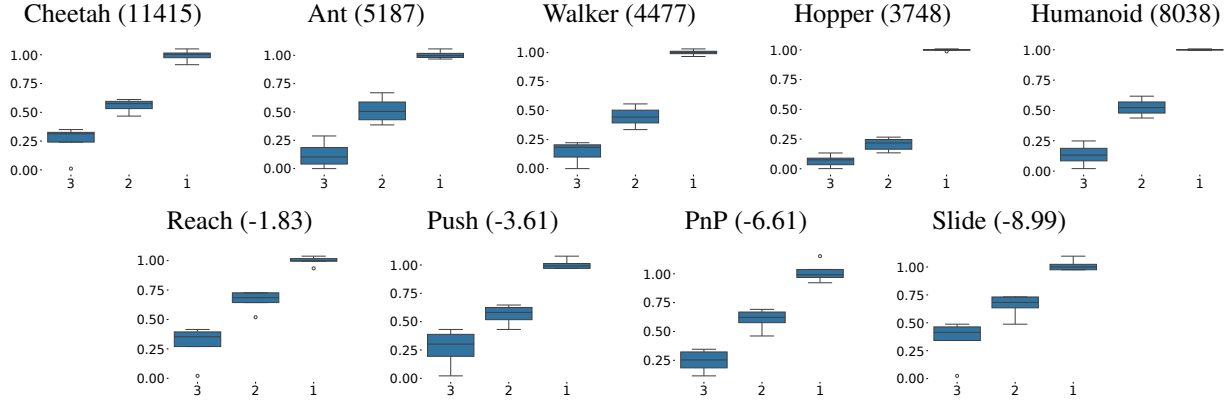


Figure 6: Whisker plots illustrate the average returns of both expert and non-expert datasets in nine distinct environments in Mujoco and Panda-gym. The numerical values following the task names represent the actual mean return of the expert policy.

B.4. More details on the Impact of Sub-optimal Datasets

In the Figure 7 we show the evaluation curves with varied sizes for sub-optimal datasets. It can be seen that the overall performance tends to improve with more sup-optimal datasets. In particular, for the Ant task, our sub-IQ even fails to maintain stability when the sizes of sup-optimal datasets are low (10k-5k-1k). Moreover, while BC seems to show improvement with more sub-optimal data, the performance of DWBC and DemoDICE remains unchanged. This may be because these approaches rely on the assumption that expert demonstrations can be extracted from the sub-optimal data, which is not the case in our context.

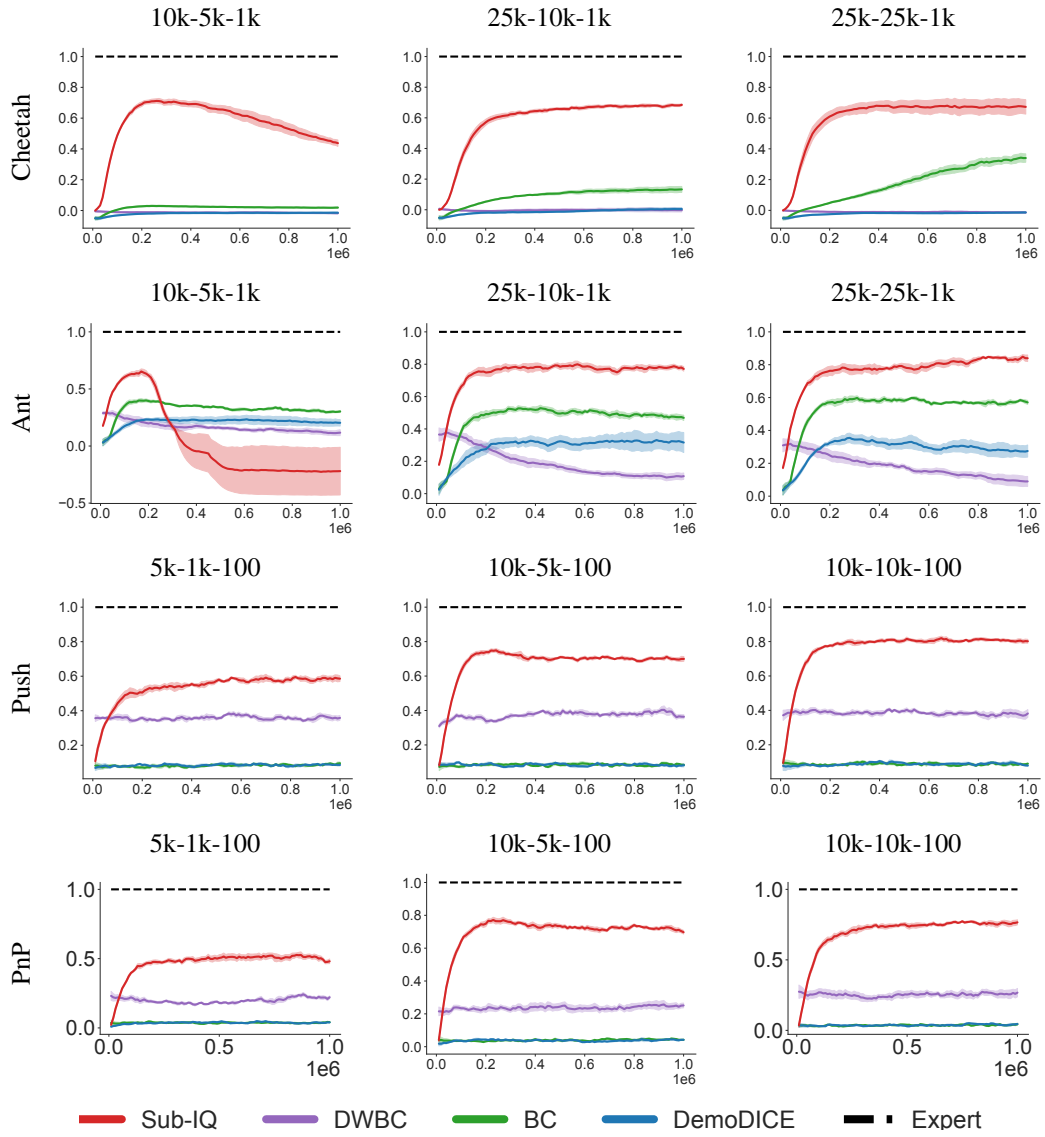


Figure 7: Evaluation curves with different sub-optimal-dataset size.

B.5. Varied Expertise Levels

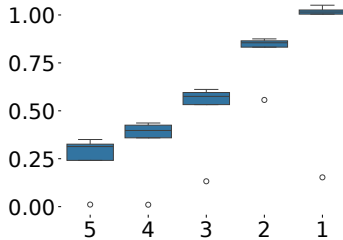


Figure 8: Average returns of the 5 *HalfCheetah* datasets (one expert and 4 non-expert).

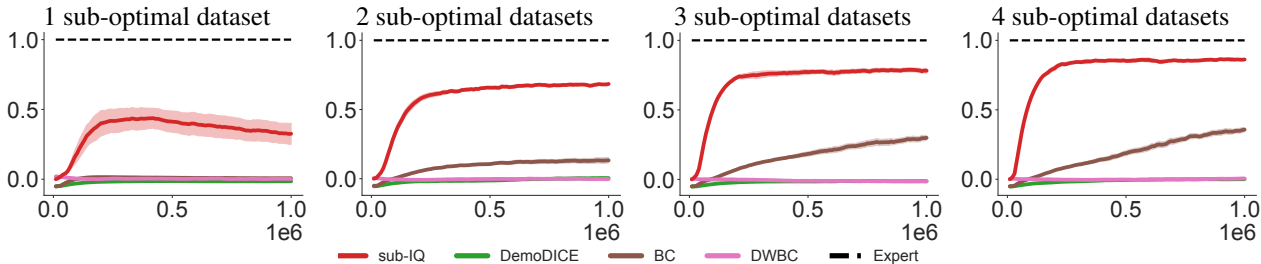


Figure 9: Experiment results for different numbers of sub-optimal datasets. The learning curves are calculated by mean with shaded by the standard error of 5 data seeds.

We assess our algorithm with different numbers of expertise levels to investigate how adding or removing sub-optimal expertise levels influences performance. Specifically, we keep the same expert dataset comprising 1 expert trajectory and conduct tests with 1 to 4 sub-optimal datasets from the Cheetah task. Details of the average returns of the five datasets are reported in Fig. 8. In this context, Sub-IQ outperforms other algorithms in utilizing non-expert demonstrations. Furthermore, BC successfully learns and achieves performance comparable to the performance of sub-IQ with 2 dataset, while DemoDICE and DWBC struggle to learn. The detailed results are plotted in Figure 9. In Section (B.7) below, We particularly delve into the situation of having two datasets (one expert and one sub-optimal), which is a typical setting in prior work.

B.6. Reward Reference Distribution

From the experiment reported in Table 1, we plot the distributions of the reward reference values in Figure 10, where the x -axis shows the level indexes and the y -axis shows reward values. The rewards seem to follow desired distributions, with larger rewards assigned to higher expertise levels. Moreover, rewards learned for expert demonstrations are consistently and significantly higher and exhibit smaller variances compared to those learned for sub-optimal transitions.

B.7. Two Dataset Training

In this experiment, we aim to test whether our algorithm is able to learn with only two datasets (one expert and one sub-optimal), which is the main setting of DemoDICE and DWBC. Here, due to the lack of other levels, we increase the dataset size of the Cheetah task (from 10k to 15k) and Ant task (from 10k to 25k) for all the approaches. Please note that although we increase our dataset sizes, they are still sufficiently smaller than the sizes of the supplementary dataset used in the aforementioned approaches (over 1,000,000 transitions). The performance is reported in Figure 11. Our sub-IQ remains significantly better than DemoDICE and DWBC. However, as our method lacks additional levels, it only achieves a performance close to sub-optimal. In the case of DWBC and DemoDICE, they are unable to harness information from the sub-optimal data, resulting in poor performance.

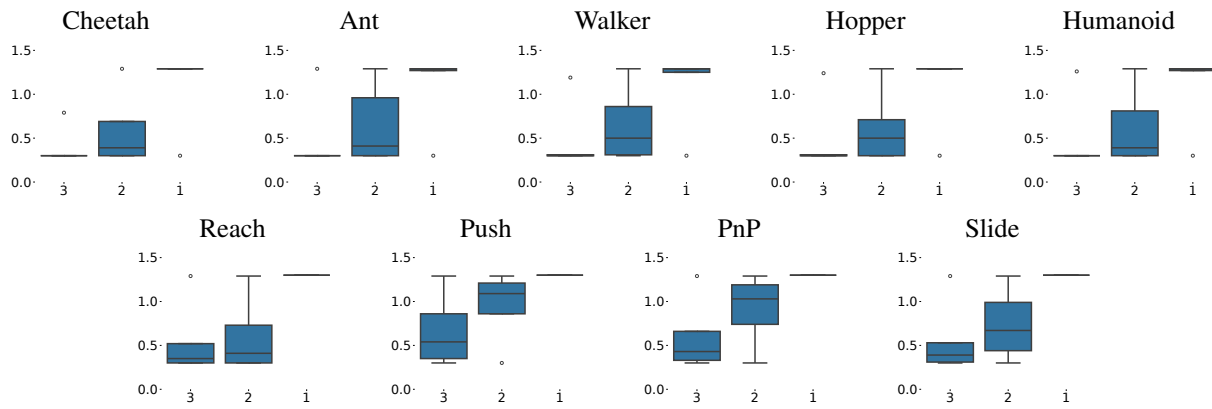


Figure 10: Whisker plots illustrate the reward reference distribution of three datasets of each environment.

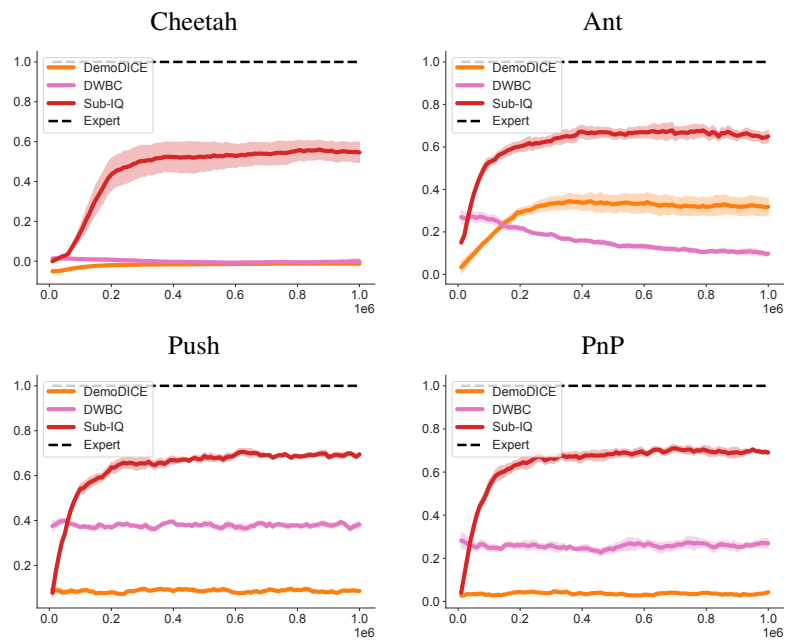


Figure 11: Two dataset experiments.

B.8. Hyper Parameters

We conducted all experiments on a total of 8 NVIDIA RTX A5000 GPUs and 96 core CPUs. We use 1 GPUs and 12 core CPUs per task with approximately one day per 5 seeds. The detailed hyper-parameters are reported in Table 2.

Table 2: Hyper parameters.

HYPER PARAMETER	BC-BASED	SUB-IQ
ACTOR NETWORK	[256,256]	[256,256]
CRITIC NETWORK	[256,256]	[256,256]
TRAINING STEP	1,000,000	1,000,000
GAMMA	0.99	0.99
LR ACTOR	0.0001	0.00003
LR CRITIC	0.0003	0.0003
LR REWARD REFERENCE	0.0003	0.0003
BATCH SIZE	256	256
w (FOR THREE EXPERTISE LEVELS)	[0.3,0.5,0.7]	[0.3,0.5,0.7]